

Regionalization of precipitation and the spatiotemporal distribution of extreme precipitation in southwestern China

L. Liu¹ · Z. X. Xu^{1,2}

Received: 11 June 2015 / Accepted: 10 October 2015 / Published online: 22 October 2015
© Springer Science+Business Media Dordrecht 2015

Abstract Daily precipitation data from 1951 to 2010 at 33 meteorological stations in five provinces/cities, including Sichuan Province, Yunnan Province, the Guangxi Zhuang Autonomous Region, Guizhou Province and Chongqing City, are used to partition the study area based on precipitation and analyze the spatiotemporal distribution of extreme precipitation. The rotated empirical orthogonal function (REOF) analysis method is used to divide the study area into five parts according to precipitation. The precipitation exhibited greater fluctuations in the last two decades. This finding indicates that extreme precipitation events are increasing. The frequent occurrence of extreme precipitation has made drought and flood disasters more serious. The Mann–Kendall test (M–K test) and moving *t* test methods are used to analyze the jump and monotonic trends of extreme precipitation indices. It is determined that extreme precipitation indices, including Rx1d, Rx5d, R95p, R99p, CWD and R10 mm, exhibited a weak upward trend during the past 60 years, suggesting that the precipitation amount in the study area decreased slightly, but the maximum daily precipitation amount (Rx1d) and the extremely wet day precipitation (R99p) increased. This finding indicates that precipitation is more concentrated and the extreme precipitation is more serious. The jump for most of the extreme precipitation indices occurred in the 1990s. In terms of spatial scale, extreme precipitation indices, except CDD and CWD, exhibited an increasing trend from the northwest to the southeast. The regions with especially high or low values are easy to identify. Drought risk in northwest Sichuan and the junction of Sichuan and Yunnan is higher. Guangxi Zhuang Autonomous Region and southern part of Yunnan Province have a higher flood risk. The trends of nine extreme precipitation indices also demonstrated the spatial differences. There are more stations exhibiting upward trends than stations showing downward trends

✉ Z. X. Xu
zongxuexu@vip.sina.com

¹ College of Water Sciences, Beijing Normal University, Xijiekouwai Street 19, Beijing 100875, People's Republic of China

² Joint Center for Global Change Studies (JCGCS), Beijing 100875, People's Republic of China

for six extreme precipitation indices. The risk of drought/flood may increase in Yunnan and Guangxi, and the storm flood risk in Chongqing exhibited an increasing trend.

Keywords Extreme precipitation indices · Spatiotemporal distribution · Regionalization · M–K test · Moving t test · REOF · Southwestern region

1 Introduction

Climate change is one of the greatest environmental events that humankind is facing in the twenty-first century. Global warming is an indisputable fact. The global mean surface temperature data exhibit an increase of approximately 0.85 °C (0.65–1.06) over the period of 1880–2012. The rate of warming over the past 62 years (1951–2012) was 0.12 °C (0.08–0.14) per decade. Each of the past three decades has been warmer than all the previous decades in the instrumental record, and the decade of the 2000s has been the warmest (IPCC 2013; Qin et al. 2014). The daily maximum and minimum temperatures increased by 0.13 and 0.32 °C, respectively, every 10 years from 1955 to 2000 in China (Liu et al. 2004; Ding et al. 2007). This finding indicates that there is an increasing trend in the frequency of extreme precipitation. Disasters attributable to extreme precipitation, such as floods and droughts, are increasing (Bates et al. 2008; Min et al. 2011). Globally, literature related to the field of climate change has provided data from trend analyses of precipitation variables (Xu et al. 2003; Su et al. 2008; Guo et al. 2011; Liu et al. 2011; Unal et al. 2012; Du et al. 2014; Thibeault and Seth 2014; Manhique et al. 2015; Tack et al. 2015; Zhang et al. 2015). The intensity and frequency of extreme precipitation events in China have shown distinct regional and seasonal characteristics in recent years.

The five southwestern provinces/cities have divergent distributions from the center of Sichuan Basin. The main climate type in this region is a subtropical monsoon climate with warm, dry winters and hot, rainy summers. It is a relatively water-rich area, but the spatial and temporal distribution is uneven. Agricultural fields are located in high places, where as irrigation water is located in the lowlands. The population in this region is scattered. Due to the impact of global climate change, the frequency and intensity of extreme climate events are increasing, especially the drought from September 2009 to March 2010, which lasted more than 6 months and was the most serious and longest continuous drought in the region on record. Therefore, studies on extreme climate events and their evolution are particularly urgent in southwestern China. This study aims to investigate the spatiotemporal trend of extreme precipitation and regionalization in the southwest region using the nonparametric M–K trend test, the moving t test and the REOF analysis, which may provide valuable feedback for policy makers to make rational use of regional water resources and to ensure the prevention and mitigation of disasters resulting from extreme precipitation events.

2 Study area and data description

The study was conducted in five provinces/cities, including Sichuan, Yunnan, Guangxi, Guizhou and Chongqing, in southwestern China. The data were retrieved from the China Meteorological Data Sharing Service System and were composed of an observed daily precipitation data series from 1951 to 2010 at 33 meteorological stations. The distribution

of the meteorological stations is shown in Fig. 1. Simple quality control was performed for the data to eliminate the impact due to missing records or station relocations. For example, the station was replaced by the Shapingba station after January 1987.

3 Methodology description

3.1 Extreme precipitation indices

The purpose of this study is to quantify the variation of extreme precipitation in the five southwest provinces/cities from 1951 to 2010. The Expert Team on Climate Change Detection and Indices (ETCCDI) jointly proposed by the Commission for Climatology (CCI)/Climate Variability and Predictability (CLIVAR) /Joint WMO-IOC Technical Commission for Oceanography and Marine Meteorology (JCOMM) is used to conduct this research. Nine extreme precipitation indices are chosen to analyze and discuss the spatiotemporal variation of the extreme precipitation; the descriptions of the indices are shown

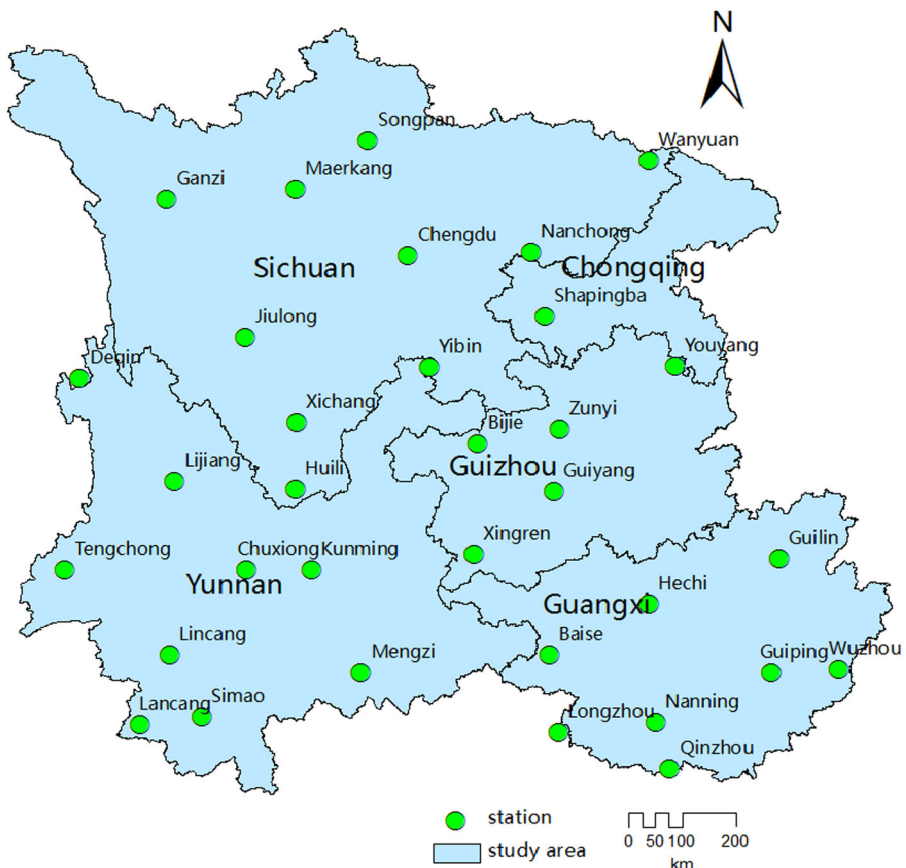


Fig. 1 Map of the study area and the meteorological stations

Table 1 Extreme precipitation indices

Index	Unit	Descriptive name	Definition
PRCPTOT	mm	Wet day precipitation	Annual total precipitation from wet days
Rx1d	mm	Maximum 1-day precipitation	Annual maximum 1-day precipitation
Rx5d	mm	Maximum 5-day precipitation	Annual maximum consecutive 5-day precipitation
R95p	mm	Very wet day precipitation	Annual total amount when PRCP > 95th percentile of 1961–1990 daily precipitation
R99p	mm	Extremely wet day precipitation	Annual total amount when PRCP > 99th percentile of 1961–1990 daily precipitation
SDII	mm/d	Simple daily intensity index	Average precipitation on wet days
CDD	d	Consecutive dry days	Maximum number of consecutive days with RR < 1 mm
CWD	d	Consecutive wet days	Maximum number of consecutive days with RR ≥ 1 mm
R10 mm	d	Heavy precipitation days	Annual count of days when PRCP ≥ 10 mm

in Table 1 (Karl et al. 1999; Zhang et al. 2005a, b; You et al. 2008). The indices are calculated by using the RCLimDex1.0, which was developed by the Climate Research Branch of the Meteorological Service of Canada (Zhang et al. 2005a, b).

Nine extreme precipitation indices at 33 stations are calculated. The average extreme precipitation indices are calculated by the mean precipitation of the 33 stations.

3.2 Nonparametric trend test

The nonparametric M–K trend test is used to analyze the trends of the extreme precipitation indices for the 33 stations. The calculation is relatively simple and can determine the beginning time of the mutation. To perform the test, Kendall’s S_k is calculated by the series of (X_n) , and the data length is n . S_k is given as:

$$S_k = \sum_{i=1}^k r_i \tag{1}$$

where $k = (2,3,\dots,n)$, S_k is the cumulative number when the i th value is greater than the j th value, and $j = (1, 2, \dots, i)$.

Assuming that the time series is random and a nonautocorrelation, then UF_k is defined as

$$UF_k = \frac{[S_k - E(S_k)]}{\sqrt{\text{Var}(S_k)}} \tag{2}$$

where $k = (2, 3, \dots, n)$, $UF_1 = 0$, and $E(S_k)$ and $\text{Var}(S_k)$ are the mean and the variance of the S_k , respectively, when $|UF_k| > U_\alpha$, indicating that the series shows an increasing or decreasing trend. All the UF_k s will form a curve UFK , which can be used to obtain the anti-series curve, UBK . If UFK is greater than 0, then the series shows an increasing trend, and if UFK is less than 0, then the series shows a decreasing trend. If UFK and UBK intersect, and the intersection is in the boundary line between the UFK and UBK , then the

moment corresponding to the intersection is the start time of the mutation (Huang and Xu 2009; Cai et al. 2012; Wang et al. 2014; Da Silva et al. 2015).

3.3 Moving *t* test

The moving *t* test method is used to examine mutation by determining whether two sample means have a significant difference. After choosing two subsequences of a time series, if the difference of their mean reaches a certain significance level, then this indicates that an abrupt change occurred.

One moment is set to be a reference point in time series “*x*” with a sample size “*n*.” The two subsequences before and after the reference point were defined to be *x*₁ and *x*₂.

$$t = \frac{\bar{x}_1 - \bar{x}_2}{s \times \sqrt{\frac{1}{n_1} + \frac{1}{n_2}}} \tag{3}$$

where

$$s = \sqrt{\frac{n_1 s_1^2 + n_2 s_2^2}{n_1 + n_2 - 2}} \tag{4}$$

*n*₁, *n*₂—the sample size of *x*₁ and *x*₂, respectively.

\bar{x}_1 , \bar{x}_2 —the average of *x*₁ and *x*₂, respectively. *s*₁², *s*₂²—the variance of *x*₁ and *x*₂, respectively. If $|t| < t_\alpha$, there is no significant difference between the two subsequences. Otherwise, there is an abrupt change at the reference point (Wei 1999).

Equation (3) follows a *t* distribution with $t = n_1 + n_2 - 2$ degrees of freedom. Because the choice of the subsequence length is artificial, the mutation point may drift; therefore, repeatedly changing the length of the subsequence is performed to enhance the reliability of the test results. 3a, 4a, 7a, 10a are chosen in this paper, respectively.

3.4 REOF analysis

Empirical orthogonal function (EOF) analysis finds linear combinations of the measured variables so that the leading EOF describes the spatially coherent equation that maximizes its variance. However, sometimes high-order EOFs have smaller spatial scales and are not physically meaningful because of orthogonality. To avoid degeneracy, rotated EOFs can be obtained using the varimax rotation (Richman 1986).

REOF yields localized structures by compromising some of the EOF properties, such as orthogonality. The effect of the rotation to simple structure is to cluster within each mode a small number of high-valued variables and a large number of near-zero value variables. REOF was found to be better in dividing climatic patterns in a comparison study (Kim and Wu 1999). In this paper, the varimax REOF method was chosen, which maximizes the variance of the squared correlation between each rotated principal component and each variable to provide the simplest pattern description while explaining the maximum amount of variance.

Assuming *X* is the data matrix of *M* × *N*, where *N* is the number of locations and *M* is the number of observations at each location. Next, the EOFs are found by determining the eigenvectors of the covariance matrix *C*, which is

$$C = \frac{1}{M} XX^T \quad (5)$$

C is an $N \times N$ real, semidefinite matrix and can therefore be written as

$$C = E\Lambda E^T \quad (6)$$

where Λ is a diagonal matrix whose elements are the N eigenvalues of C , and E is an orthogonal matrix whose columns are the N orthogonal eigenvectors, i.e., EOFs. Each EOF has a corresponding time series, so-called principal components (PCs), and the two satisfy

$$X = PE \quad (7)$$

where P is an $M \times N$ matrix whose columns are the N PCs. Combining Eqs. (5), (6), and (7), we obtain

$$\Lambda = \frac{1}{M} P^T P \quad (8)$$

Because Λ is diagonal, the PCs are mutually orthogonal and the eigenvalues are equal to their variances.

An $m \times m$ rotation matrix Q is used to construct the rotated EOFs U , according to

$$U = EQ \quad (9)$$

Here, $E = [E_1, E_2, \dots, E_m]$, which is the matrix of the leading m EOFs. The orthogonal rotation Q is chosen to be orthogonal.

$$QQ^T = I \quad (10)$$

The varimax criterion is the most popular orthogonal rotation scheme because of the following criterion (Kaiser 1958):

$$\max \left(\sum_{k=1}^m \left[\frac{1}{p} \sum_{j=1}^p u_{jk}^4 - \frac{1}{p^2} \left(\sum_{j=1}^p u_{jk}^2 \right)^2 \right] \right) \quad (11)$$

where $U = (u_{ij})$ and m is the number of EOFs chosen for rotation. In this criterion, the simplicity of the complete factor matrix is defined as the maximization of the sum of the simplicities of the individual factors (Li et al. 2009).

4 Results analysis and discussion

4.1 Precipitation features and regionalization

Precipitation of the Qinzhou station in Guangxi is 2112 mm, which is the highest value in the 33 stations. The minimal precipitation is only 622 mm at the Ganzi station of Sichuan. The precipitation distribution in southwestern China is uneven, which shows an increasing trend from the northwest to the southeast. Overall, precipitation in Guangxi is the highest in the study area, whereas Sichuan Province has the lowest. The REOF analysis method is used to partition the study region according to precipitation.

The eigenvalues associated with the EOF series can be used to determine the proportion of the total variance explained by each series. The results indicate that the first 6 EOFs together explain 83.70 % of the variance. The fact that more than 80 % of the total variability has been captured in the first 6 EOFs indicates that the complexity of spatial pattern of precipitation over southwestern China can largely be explained by a small number of spatial structures. Rotating the first six loading vectors of the initial EOFs produces a new set of REOF modes (Table 2).

Figure 2a₁ shows the first mode, accounting for 24.88 % of the total variance; although the value is small, it is the maximum of the first 6 modes (Table 2). The first mode is the most common mode for the precipitation distribution in southwestern China. The high load (RLV value > 0.6) region is located in the south of Yunnan Province and much of Guangxi Zhuang Autonomous Region (region I), which includes the Qinzhou, Longzhou, and Kunming stations, of which the Longzhou station has the highest RLV value of 0.82. Figure 2a₂ shows the second mode, accounting for 17.24 % of the total variance. The high load area is located in the northwest of Sichuan Province (region II), which includes the Maerkang and Jiulong stations, of which the Maerkang station has the highest RLV value of 0.79. Figure 2a₃ shows the third mode, which is highlighted in Chongqing City and Guizhou Province (region III), which includes the Guiyang and Youyang stations, with RLV values of 0.75 and 0.79, respectively. Figure 2a₃ also shows another high load region located at the junction of Sichuan Province and Yunnan Province (region IV), including the Huili station, with an RLV value of 0.63. The remaining district in the east of Sichuan Province is region V.

Figure 2b₁ is the time coefficient corresponding to the first mode. Because RLV1 values are positive, the peak (valley) values of the time coefficient curve correspond to years with more (less) precipitation. Typical rainy years of regions II, III, and IV are, respectively, 2010, 2009, and 2009, whereas the typical drought years are 2009, 1996, and 1996. 1996 is a typical rainy year of region I, whereas 1985 is a typical drought year. The time coefficients (Fig. 2b₁, b₂, b₃) of the three modes show that the annual variation of precipitation is not significant before the middle 1990s; however, the variation range of precipitation increased, especially in recent years, and extreme precipitation has become more usual (Table 3).

Table 2 The explained variance and the accumulated explained variance of the first six EOF and REOF modes

Mode	EOF			REOF		
	Eigenvalues	Explained variance (%)	Accumulate explained variance (%)	Eigenvalues	Variance contribution (%)	Accumulate explained variance (%)
1	21.85	66.21	66.21	8.21	24.88	24.88
2	2.44	7.39	73.61	5.69	17.24	42.12
3	1.10	3.33	76.94	5.49	16.64	58.76
4	0.88	2.67	79.61	3.06	9.27	68.03
5	0.70	2.12	81.73	2.92	8.85	76.88
6	0.65	1.97	83.70	2.25	6.82	83.70

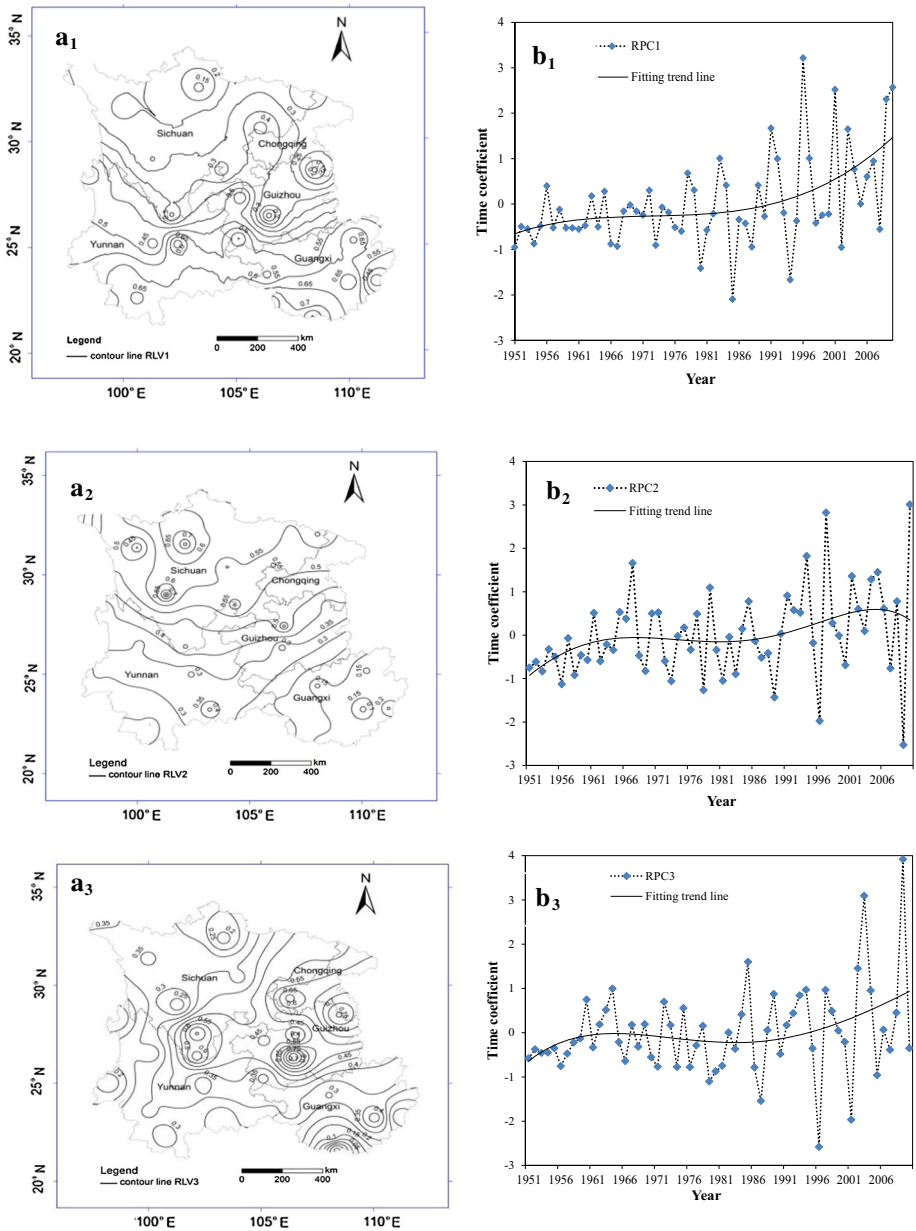


Fig. 2 The first 3 modes (**a₁**, **a₂**, **a₃**) and the corresponding time coefficient (**b₁**, **b₂**, **b₃**) of REOF analysis for precipitation in southwestern China

4.2 Changes of the extreme precipitation indices

Using the Mann–Kendall method combined with the linear trend analysis, the trend test result of the five provinces/cities is given in Table 4, which shows the M–K test statistic

Table 3 Rough regionalization of southwestern China

Number	Stations
Region I	Tengchong, Lincang, Lancang, Simao, Mengzi, Kunming, Baise, Hechi, Xingren, Nanning, Guilin, Guiping, Qinzhou, Longzhou, Wuzhou
Region II	Ganzi, Maerkang, Songpan, Jiulong
Region III	Yoyang, Shapingba, Zunyi, Bijie, Guiyang
Region IV	Huili, Xichang, Lijiang, Chuxiong, Deqin
Region V	Nanchong, Wanyuan, Chengdu, Yibin

Table 4 M–K statistic values of extreme precipitation indices of the five southwestern provinces

Index	Z	β	Trend	Jump year
PRCPTOT	-0.497	-0.420 mm/a	↓	-
Rx1d	1.467	0.036 mm/a	↑	1962
Rx5d	0.714	0.026 mm/a	↑	1996
R95p	1.390	0.674 mm/a	↑	1993
R99p	2.405	0.571 mm/a	↑	-
SDII	-0.096	0 mm/a	-	-
CDD	-0.880	-0.124 d/a	↓	-
CWD	0.727	0.116 d/a	↑	1993
R10 mm	0.364	0.013 d/a	↑	2002

values. Wet day precipitation (PRCPTOT) of the five southwestern provinces/cities showed a small downward trend, with a linear trend of -4.204 mm/10a. The 5-year moving average method and the Mann–Kendall trend test method are used to analyze the time series, as shown in Figs. 3a and 4a, respectively. There are multiple intersections of the curve Ufk and UBk with Fig. 3a, indicating that there may be several mutations of the PRCPTOT series. However, the result of the moving t test and 5-year moving average with Fig. 4a showed cyclical fluctuations for PRCPTOT. The overall trends of Rx1 day and Rx5 day are not obvious, as shown in Figs. 3b, c, respectively; the linear trends are 0.362 and 0.262 mm/10a, respectively. Figure 4b and 4c shows a few intersections of Ufk and UBk, and combined with the analysis of the moving t test method, the mutations of Rx1 day and Rx5 day were determined to occur in 1962 and 1996, respectively. Rx1d has been showing an upward trend after 1962, while the Rx5d is fluctuating.

R95p of the five provinces/cities showed an increasing trend on the whole, with a linear trend of 6.739 mm/10a. Figure 4d shows that three intersection points occurred between 1990 and 1993, and combined with the analysis of the 5-year moving average curve (Fig. 3d) and moving t test, the mutation of R95p was determined to occur in 1993. R99p also showed an obvious increasing trend, with a linear trend of 5.713 mm/10a. Through the analysis of moving t test method, the only one intersection point showed in Fig. 4e is not the jump year. R99p has been showing an upward trend after the 1960s.

The overall linear trend of the simple precipitation intensity index (SDII) is almost 0 mm/10a. The SDII showed an upward trend at the beginning of the 1950s, followed by a weak downward trend, but it showed cyclical fluctuations in the whole period (Figs. 3f, 4f). Figure 4f shows two intersections at 1952 and 1999 of Ufk and UBk, but they were

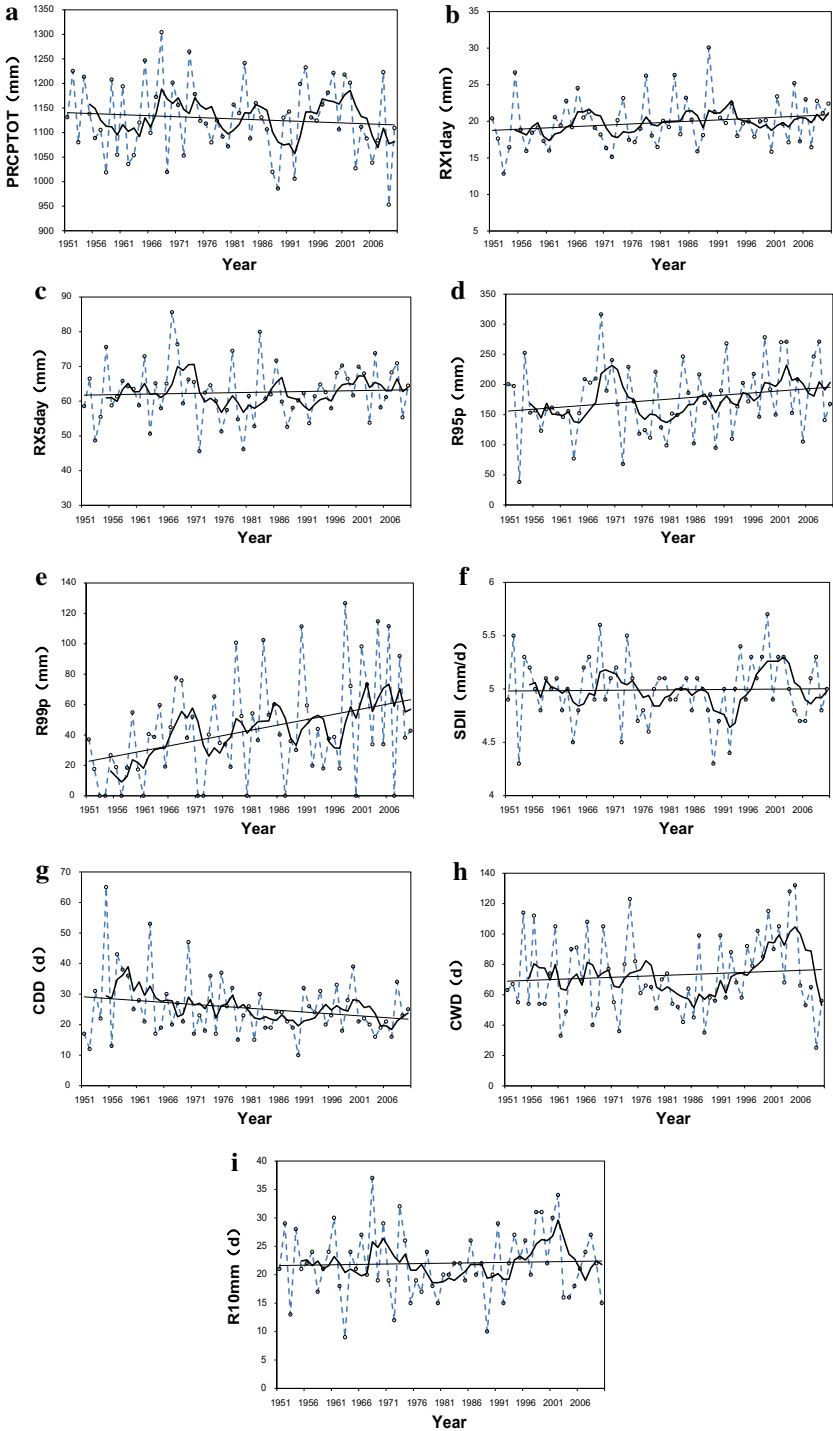


Fig. 3 Trend of the extreme precipitation indices of the five southwestern provinces during 1951–2010. (The *dashed line* shows the measured value, the *thin solid line* is the linear trend, and the *thick solid line* is a 5-year moving average.) **a** Wet day precipitation, **b** maximum 1-day precipitation, **c** maximum 5-day precipitation, **d** very wet day precipitation, **e** extremely wet day precipitation, **f** simple daily intensity index, **g** consecutive dry days, **h** consecutive wet days, **i** heavy precipitation days

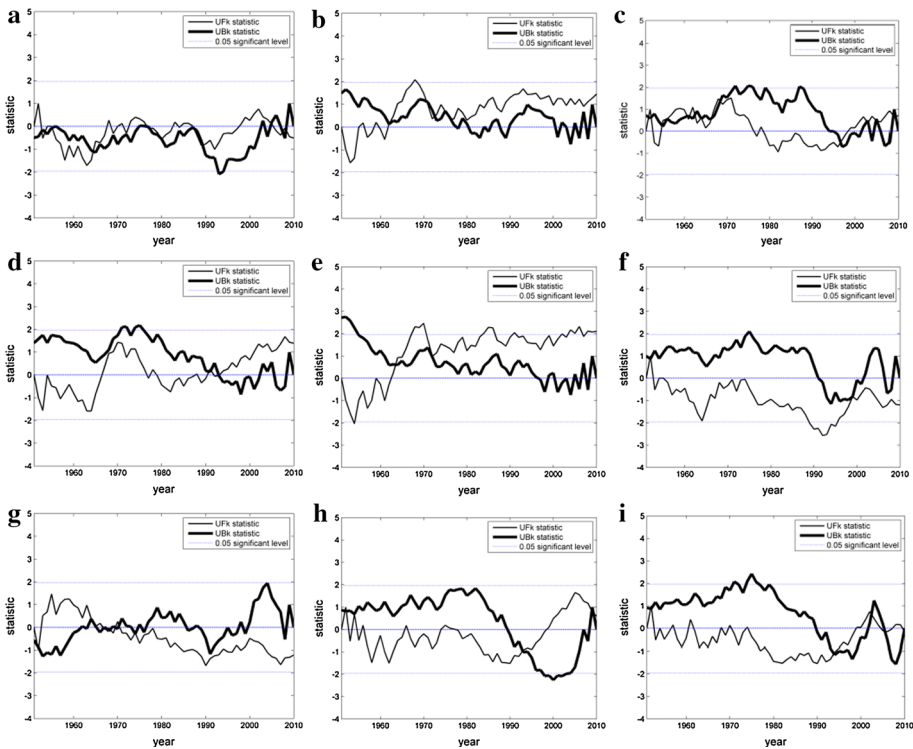


Fig. 4 Mann–Kendall jump test of extreme precipitation indices of the five southwestern provinces during 1951–2010. **a** PRCPTOT, **b** Rx1day, **c** Rx5day, **d** R95p, **e** R99p, **f** SDII, **g** CDD, **h** CWD, **i** R10 mm

determined to be not the jump year through verification of the moving *t* test method and 5-year moving average.

CDD showed a decreasing trend (Figs. 3g, 4g), with a linear trend of $-1.238 \text{ mm}/10\text{a}$ as a whole; however, it showed an increasing trend before the 1970s followed by a decreasing trend. There are some intersections of UFk and UBk between the mid-1960 and 1970s, but there is no significant jump year according to the moving *t* test method. CWD showed an increasing trend in the whole period, and the linear trend is $1.16\text{d}/10\text{a}$. CWD showed a fluctuating trend before the 1980s, and then, it showed a downward trend until 1993; then, it showed a significant increasing trend. Figure 4h shows three intersections of UFk and UBk, while only 1993 is the jump year through verification of the moving *t* test method.

PRCPTOT showed weak downward trends during the past 60 years, whereas Rx1d, Rx5d, R95p, and R99p increased. This indicates that the precipitation is more concentrated, and the amount of precipitation during individual events is increasing. At the same

time, it can be summarized that extreme precipitation occurred more frequently. Most of the jump years occurred in the 1990s, and it indicates large changes occurred in extreme precipitation after the 1990s.

4.3 Spatial distribution of extreme precipitation indices

Figure 5 shows the distribution of the nine extreme precipitation indices of the southwestern provinces/cities. PRCPTOT, Rx1d, Rx5d, R95p, and R99p show increasing trends from the northwest to the southeast, and the distribution of higher values and lower values is obvious. Some stations in Guangxi Zhuang Autonomous Region and southern of Yunnan Province have high values. PRCPTOT at the Qinzhou station in Guangxi Zhuang

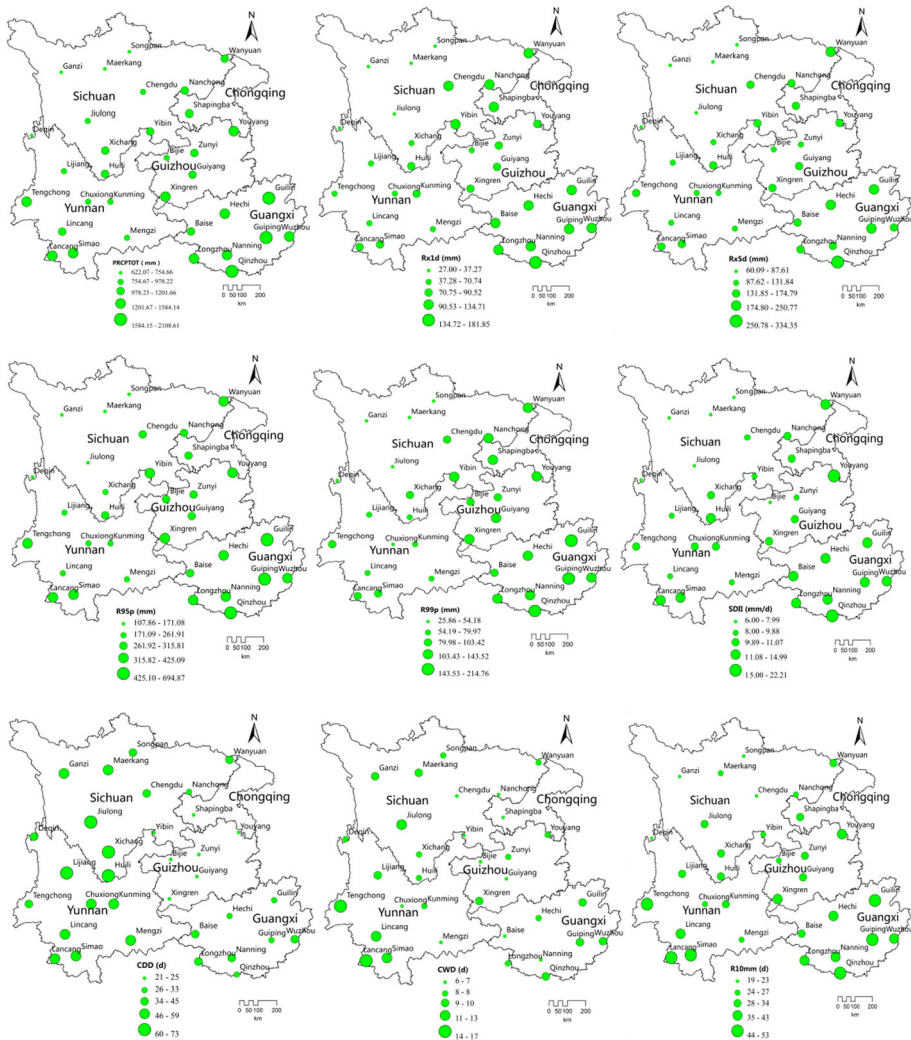


Fig. 5 Spatial distribution of extreme precipitation. The different panels show different indices

Autonomous Region is more than 2000 mm, and the values of the Guilin, Guiping, and Lancang stations in Yunnan are also more than 1500 mm. Rx1d, Rx5d, R95p, and R99p at the Qinzhou, Guilin, and Guiping stations are also high, with values greater than 120, 200, 510, and 180 mm, respectively. Qinzhou station showed the highest values of PRCPTOT, Rx1d, Rx5d, R95p, and R99p. The low value area is in Sichuan Province; PRCPTOT, Rx1d, Rx5d, R95p, and R99p at the Ganzi, Songpan, Maerkang, Jiulong, and Deqin stations, which are located near the junction of Yunnan and Sichuan Provinces, are less than 800, 40, 90, 180, and 50 mm, respectively. The values of these five indices in Chongqing City and Guizhou Province are at a moderate level.

The spatial distribution of SDII also shows an increasing trend from the northwest to the southeast. The lower value area is in Sichuan Province and the juncture of Sichuan and Yunnan, where the mean daily rainfall intensity is below 8 mm/d. SDII in the south of Yunnan and Guangxi Zhuang Autonomous Region is more than 12 mm/day, and the maximum value is at the Youyang station (22.21 mm/day), located at the juncture of Guizhou and Chongqing.

CDD shows a decreasing trend from the west to east; CDD in Yunnan and the south of Sichuan is over 50 days, and the highest value is 73 days at the Lijiang station. Lijiang station is located in the northwest of Yunnan, near the junction of Sichuan and Yunnan Provinces. The uneven distribution of precipitation over the year is the main reason for great CDD values. CDD in Guizhou Province and Chongqing City is less than 25 days, and other indices here are at a moderate level or at a high level, so the drought risk in this region is lower.

CWD showed no obvious trend in spatial distribution. The value of CWD in southwestern Yunnan is greater, because the southern subtropics mountainous area has monsoon climate with wet summer and dry winter. CWD in Jiulong station is higher due to rainy summer, which is caused by the complex terrain and big difference in altitude, but other indices in this station are at a moderate level, so the flood risk at Jiulong station is not high.

R10 mm shows an increasing trend from north to south. R10 mm in southern Yunnan and Guangxi Zhuang Autonomous Region is over 40 days, and the highest value is 53 days at the Lancang station.

The results showed that generally, there was an increasing trend in precipitation from the northwest to the southeast in the southwestern five provinces/cities. This is supported by the existing studies (Yuan et al. 2014). The extreme precipitation indices, except CDD in junction of Yunnan and Sichuan, were at a middle level (CDD was at a high level), which indicates that the drought in the region is more severe. The CDD in northwest Sichuan was also at a high level, with very low precipitation. The drought risk in northwestern Sichuan is severe. This is in accordance with existing studies and the actual situation (Wang et al. 2012) The PRCPTOT, R1d, R5d, R95p, R99p, and R10 mm in Guangxi Zhuang Autonomous Region and southern part of Yunnan Province were at a high level, while the CDD and CWD were at a moderate level, indicating a higher flood risk. Southwestern China is impacted by monsoon activities and landforms; although precipitation is abundant, most of the rainfall infiltrates and flows away in karst landforms, with large height differences and steep slopes. Water resources are thus more difficult to obtain. Precipitation is inhibited to some extent due to the obvious influence of Indian Ocean convection. Chinese scholars also have the same point of view (Zhang et al. 2013; Yuan et al. 2014).

4.4 Spatial distribution for the long-term trend of extreme precipitation indices

The linear trend values at 33 stations were used to construct a map to illustrate the spatial distribution trend of extreme precipitation of the five southwestern provinces/cities (Fig. 6). Figure 6 shows that there were obvious spatial differences of PRCPTOT, Rx1d, Rx5d, R95p, and R99p. PRCPTOT showed an increasing trend in northwest Yunnan, west Sichuan, and the Chongqing, Guilin, and Qinzhou stations in Guangxi with a linear trend between 0.004 and 3.013 mm/a. PRCPTOT at the other stations (19 stations) showed a decreasing trend, with a linear trend between -0.214 and -5.836 mm/a. It indicates that precipitation in the west of Southwestern China was increasing, while precipitation in most

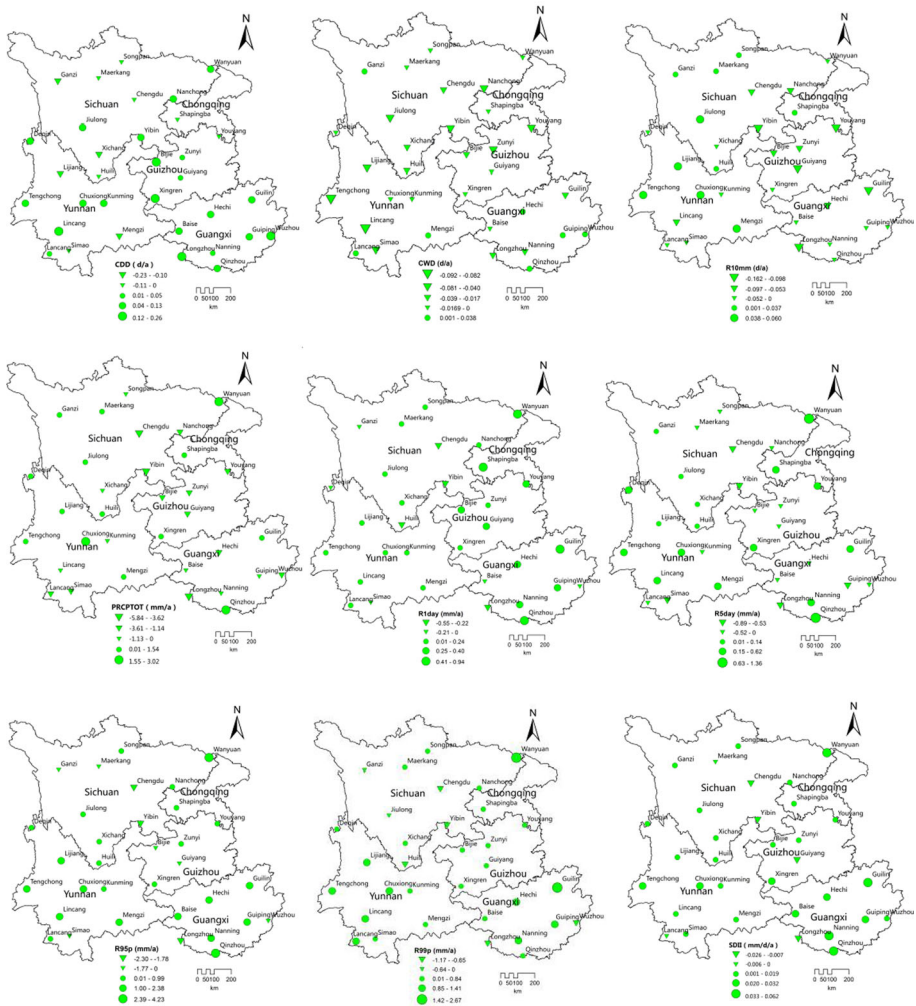


Fig. 6 Spatial distribution of extreme precipitation trends. The different panels represent different extreme precipitation indices

of the east part except Chongqing City was decreasing. This is consistent with the results of other Chinese scholars (Liu et al. 2007). The stations where Rx1d decreased were mainly in Sichuan and Guangxi. Rx1d showed downward trends at 7 stations (21.2 % of all stations), with a linear trend between -0.553 and -0.007 mm/a. As for Rx5d, the number of stations with upward trends was almost the same as that with downward trends. The largest linear trend of Rx5d was up to 1.359 mm/a at Wanyuan station located in the northeast of Sichuan Province. But the stations where Rx5d increased were mainly in Yunnan and the south of Sichuan Province. The smallest trend of Rx5d was also in Sichuan Province (Yibin station), and the linear trend was -0.89 mm/a. Only nine stations showed downward trends of R95p; these stations were distributed in Sichuan and Guizhou Province, which had linear trends between -2.306 and -0.066 mm/a. R95p at some stations in Yunnan and Guangxi Province showed an obvious increasing trend, and the linear trend at the Qinzhou station was up to 3.738 mm/a. R99p at seven stations distributed in Sichuan and Guangxi showed downward trends, with a linear trend between -1.173 and -0.095 mm/a. R99p at other stations showed upward trends, and the linear trend of the Guilin station was up to 2.670 mm/a.

Only 6 stations showed a downward trend for SDII, whereas the other 27 stations showed an upward trend, with a linear trend between 0.001 and 0.062 mm/day/a. CDD showed a slight upward trend at 23 stations, which were mainly distributed in Guizhou, Guangxi, and Yunnan. The trend was not obvious, and the linear trend was 0–0.261d/a. Twenty-six stations (78.8 % of all stations) showed a inappreciable downward trend for CWD, with a linear trend between -0.092 and -0.001 mm/a. CWD at seven stations located in Guangxi and the south of Yunnan Province showed a tiny upward trend. R10 mm showed unobvious linear trends, and the number of stations with upward trends was more than that with downward trends. R10 mm showed upward trends at ten stations, which were mainly located in the northwest of Sichuan and the north of Yunnan Province. It showed an upward trend at 23 stations, with the linear trend between -0.162 and -0.008 d/a.

Rx1d, Rx5d, R95p, R99p, SDII, and CDD at most stations in Yunnan and Guangxi showed upward trends, whereas PRCPTOT at most stations showed decreasing trends, indicating increasing short-duration precipitation events and more concentrated precipitation, additionally, the risk of drought/flood in Yunnan and Guangxi may increase. CDD and CWD in Chongqing City showed a decreasing trend, whereas the other indices showed an increasing trend, indicating an increasing storm flood risk in Chongqing City.

5 Conclusions

From the above analysis, regionalization of precipitation and the spatiotemporal distribution of extreme precipitation in the southwest provinces/cities are obtained, and the following conclusions can be summarized:

1. The REOF method is used to divide southwest China into five regions on the basis of precipitation: south of Yunnan Province and the Guangxi Zhuang Autonomous Region, northwest Sichuan Province, Chongqing City and Guizhou Province, the junction of north of Yunnan Province with Sichuan Province, and the east of Sichuan Province. The southern Yunnan Province and the Guangxi Zhuang Autonomous Region is a typical region of the precipitation distribution in the study area. The time coefficients indicate that the amplitude of precipitation variation in southwestern

- China has been increasing for nearly 20 years and that extreme values have also increased. The occurrence of extreme precipitation events increases the likelihood and severity of drought and flood disasters.
2. Over this timescale, most extreme precipitation indices showed weak upward trends over the last 60 years; however, PRCPTOT and CDD showed nonsignificant downward trends. This finding indicates that the total precipitation in the study area is decreasing, but the concentration of the precipitation is increasing, and the maximum daily rainfall and the intensity of rainfall are increasing. This is confirmed by the increase in R95, Rx1d, Rx5d, and SDII. Most of the jump years occurred in the 1990s.
 3. The spatial distribution of long-term trend of most extreme precipitation indices showed an increasing trend from the northwest to the southeast, and the regions with particularly high or low values are easy to determine. Precipitation conditions in Guangxi, Guizhou, and Chongqing Provinces/Cities are better than those in northwest Sichuan and the junction of Sichuan and Yunnan, although CDD showed a high value. Therefore, drought risk in northwest Sichuan and the junction of Sichuan and Yunnan Province is higher. The CDD and CWD in Guangxi Zhuang Autonomous Region and southern of Yunnan Province were at a moderate level, while the other indices were at a high level, indicating a higher flood risk in this region.
 4. The trends of six extreme precipitation indices also showed spatial differences. There are more stations showing upward trends than stations showing downward trends for the five extreme precipitation indices, except for PRCPTOT. Yunnan and Guangxi showed increasing short-duration precipitation and more concentrated precipitation, suggesting that the risk of drought/flood events may increase. CDD in Chongqing City showed a decreasing trend, but all other indices increased. This indicates that the flood risk in Chongqing city has increased.

Acknowledgments The study was financially supported by the major consulting project of the Chinese Academy of Engineering (2012-ZD-2013). The authors greatly appreciate the Expert Team on Climate Change Detection, Monitoring and Indices. The authors also thank the developer of the RCLimDex software.

References

- Bates BC, Kundzewicz ZW, Wu S, Palutikof JPE (2008) Climate change and water. Technical paper of the intergovernmental panel on climate change, Geneva: IPCC Secretariat
- Cai X, Cai L, Li C, Wu Z (2012) Temporal changes and mutation analysis of precipitation in Shanxi Province. *Agric Res Arid Areas* 2:247–254 (**In Chinese**)
- Da Silva RM, Santos CAG, Moreira M, Corte-Real J, Silva VCL, Medeiros IC (2015) Rainfall and river flow trends using Mann–Kendall and Sen’s slope estimator statistical tests in the Cobres River basin. *Nat Hazards* 77(2):1205–1221
- Ding YH, Ren GY, Zhao ZC (2007) Detection, causes and projection of climate change over China: an overview of recent progress. *Adv Atmos Sci* 24(6):954–971
- Du H, Xia J, Zeng S (2014) Regional frequency analysis of extreme precipitation and its spatio-temporal characteristics in the Huai River Basin, China. *Nat Hazards* 70(1):195–215
- Guo R, Li F, He W, Yang S, Sun G (2011) Spatial and temporal variability of annual precipitation during 1958–2007 in loess plateau, China. In Li DL, Liu Y, Chen YY (eds.) *IFIP Advances in information and communication technology*, pp. 551–560
- Huang JX, Xu ZX (2009) Climate change and its evolution trend of Taihu basin in 1954–2006. *Resour Environ Yangtze Basin* 18(1):33–40 (**In Chinese**)

- IPCC (2013). Climate Change 2013: the physical science basis. contribution of working group I to the fifth assessment report of the intergovernmental panel on climate change. pp. 1–1552. Cambridge: Cambridge University Press
- Kaiser HF (1958) The varimax criterion for analytic rotation in factor analysis. pp. 187–200
- Karl TR, Nicholls N, Ghazi A (1999) Clivar/GCOS/WMO workshop on indices and indicators for climate extremes workshop summary. *Clim Change* 42(1):3–7
- Kim KY, Wu QG (1999) A comparison study of EOF techniques: analysis of non-stationary data with periodic statistics. *J Clim* 12:185–199
- Li J, Carlson BE, Laci AA (2009) A study on the temporal and spatial variability of absorbing aerosols using total ozone mapping spectrometer and ozone monitoring instrument aerosol index data. *J Geophys Res Atmos* 114(D9):D09213
- Liu BH, Xu M, Henderson M (2004) Taking China's temperature: daily range, warming trends, and regional variations, 1995–2000. *J Clim* 17(22):4453–4462
- Liu XR, Li GP, Fan GZ, Cheng BY, Li HQ (2007) Spatial and temporal characteristics of precipitation resource in southwest china during 1961–2000. *J Nat Resour* 22(5):783–792 **(In Chinese)**
- Liu XC, Xu ZX, Yu RH (2011) Trend of climate variability in China during the past decades. *Clim Change* 109(3–4):503–516
- Manhique AJ, Reason CJC, Silinto B, Zucula J, Raiva I, Congolo F, Mavume AF (2015) Extreme rainfall and floods in southern Africa in January 2013 and associated circulation patterns. pp. 679–691
- Min SK, Zhang XB, Zwiers FW et al (2011) Human contribution to more-intense precipitation extremes. *Nature* 470:378–381
- Qin DH, Stocker T, Authors and TSU (2014) Highlights of the IPCC working group I fifth assessment report. *Progressus Inquisitiones DE Mutatione Climatis* 10(1):1–6 **(In Chinese)**
- Richman MB (1986) Rotation of principal components. *J Climatol* 6(3):293–335
- Su B, Gemmer M, Jiang T (2008) Spatial and temporal variation of extreme precipitation over the Yangtze River Basin. *Quatern Int* 186(1):22–31
- Tack AJM, Mononen T, Hanski I (2015) Increasing frequency of low summer precipitation synchronizes dynamics and compromises metapopulation stability in the Glanville fritillary butterfly. *Proceedings. Biological sciences/The Royal Society*, 282(1806)
- Thibeault JM, Seth A (2014) Changing climate extremes in the Northeast United States: observations and projections from CMIP5. *Clim Change* 127(2):273–287
- Unal YS, Deniz A, Toros H, Incecik S (2012) Temporal and spatial patterns of precipitation variability for annual, wet, and dry seasons in Turkey. *Int J Climatol* 32(3):392–405
- Wang MT, Wang X, Huang WH, Zhang YF, Ma J (2012) Temporal and spatial distribution of seasonal drought in Southwest of China based on relative moisture index. *Trans Chin Soc Agric Eng* 28(19):85–92 **(In Chinese)**
- Wang X, Liang P, Li C, Wu F (2014) Analysis of regional temperature variation characteristics in the Lancang River Basin in southwestern China. *Quatern Int* 333:198–206
- Wei FY (1999) The statistics and prediction of climate. China Meteorological Press, Beijing **(In Chinese)**
- Xu ZX, Takeuchi K, Ishidaira H (2003) Monotonic trend and step changes in Japanese precipitation. *J Hydrol* 279(1–4):144–150
- You QL, Kang SC, Aguilar E, Yan YP (2008) Changes in daily climate extremes in the eastern and central Tibetan Plateau during 1961–2005. *J Geophys Res* 113:D07101
- Yuan WD, Zheng JK, Dong K (2014) Spatial and temporal variation in extreme precipitation events in southwestern china during 1962–2012. *Resour Sci* 36(4):766–772 **(In Chinese)**
- Zhang X, Hantosh TH, Albert P, Semawi M, Ali MK, Al-Oulan MHSA, Zatari T, Khelet IAD, Hamoud S, Sagir R, Aguilar E, Demircan M, Eken M, Adiguzel M, Alexander L, Peterson TC, Wallis T, Sensoy S, Melkonyan H, Tagiyeva H, Ahmed N, Kutaladze N, Rahimzadeh F, Taghipour A (2005a) Trends in middle east climate extreme indices from 1950 to 2003. *J Geophys Res Atmos* 110(D22):D22104
- Zhang X, Hegerl G, Zwiers FW, Kenyon J (2005b) Avoiding inhomogeneity in percentile-based indices of temperature extremes. *J Clim* 18(11):1641–1651
- Zhang MJ, He JJ, Wang BL, Wang SJ, Li SS, Liu WL, Ma XN (2013) Extreme drought changes in Southwest China from 1960 to 2009. *J Geog Sci* 23(1):3–16 **(In Chinese)**
- Zhang DD, Yan DH, Wang YC, Lu F, Liu SH (2015) GAMLSS-based nonstationary modeling of extreme precipitation in Beijing-Tianjin-Hebei region of China. *Nat Hazards* 77(2):1037–1053